Qi et al. Nanoscale Research Letters (2017) 12:516
DOI 10.1186/s11671-017-2284-5

Nanoscale Research Letters

NANO EXPRESS Open Access

Experimental Study on the Flow and Heat Transfer Characteristics of TiO_2-Water Nanofluids in a Spirally Fluted Tube

Cong Qi*, Chunyang Li and Guiqing Wang

Abstract

The flow and heat transfer characteristics of TiO_2-water nanofluids with different nanoparticle mass fractions in a spirally fluted tube and a smooth tube are experimentally investigated at different Reynolds numbers. The effects of pH values and doses of dispersant agent on the stability of TiO_2-water nanofluids are discussed. The effects of nanoparticle mass fractions and Reynolds numbers on Nusselt numbers and frictional resistance coefficients in the spirally fluted tube and the smooth tube are also investigated. It is found that TiO_2-water nanofluids in the spirally fluted tube have a larger enhancement than that in the smooth tube. The heat transfer enhancement and the increase in frictional resistance coefficients of TiO_2-water nanofluids in the spirally fluted tube and the smooth tube for laminar flow and turbulent flow are compared. It is found that there are a larger increase in heat transfer and a smaller increase in frictional resistance coefficients for turbulent flow than that for laminar flow of TiO_2-water nanofluids in the spirally fluted tube. The comprehensive evaluations for the thermo-hydraulic performance of TiO_2-water nanofluids in the smooth tube and spirally fluted tube are also discussed.

Keywords: Nanofluids, Spirally fluted tube, Heat transfer enhancement, Frictional resistance coefficient

Background

Nanofluids are a type of medium fluids with excellent heat transfer performance (for example ZnO-EG nanofluid [1], Cu-CTAC/NaSal nanofluid [2], MWCNTs-CTAC/NaSal nanofluid [3]), which are applied in various fields, such as clean water generation [4], solar photothermal conversion [5], and boiling heat transfer [6].

Convection heat transfer of nanofluids is an important heat transfer process including natural convection and forced convection heat transfer. Many researchers have investigated the natural convection heat transfer of nanofluids. Li et al. [7] experimentally investigated the natural convection of a square enclosure filled with ZnO-EG/DW nanofluids and obtained a conclusion that the high EG aqueous solution concentration is disadvantageous to heat transfer enhancement. Hu et al. [8] experimentally and numerically investigated the natural convection of Al_2O_3-water nanofluids in a square enclosure, and it was found that nanofluids with the highest nanoparticle fraction worsen the heat transfer. He et al. [9] numerically studied the natural convection of Al_2O_3-water nanofluids in a square enclosure by a lattice Boltzmann method, and the results showed that the heat transfer performance decreases with the nanoparticle volume fraction. Qi et al. numerically studied the natural convection of Cu-Gallium nanofluids in different aspect ratio enclosures by a single-phase model [10] and a two-phase lattice Boltzmann model [11]; they [12] also studied the natural convection of Al_2O_3-water nanofluids using a two-phase lattice Boltzmann model, and the results showed that nanofluids in a smaller aspect ratio enclosure have a higher heat transfer enhancement ratio. In conclusion, it is observed that some factors, such as high heating power and nanoparticle fraction, are advantageous to heat transfer enhancement, while some other factors, such as the big aspect ratio of enclosure and the base fluid with low thermal conductivity, may lead to a reduction in natural convection heat transfer. Although natural convection of nanofluids is widely applied in many fields, it cannot meet the high

* Correspondence: qicong@cumt.edu.cn
School of Electrical and Power Engineering, China University of Mining and Technology, Xuzhou 221116, China

efficient heat dissipation under the condition of high power density.

Compared with natural convection, forced convection heat transfer has a higher heat transfer coefficient. Researchers adopted different experimental methods to investigate the forced convection heat transfer characteristics of nanofluids. Sun et al. [13, 14] experimentally investigated the flow and heat transfer characteristics of Cu-water, Al-water, Al_2O_3-water, Fe_2O_3-water, and Cu-water nanofluids in a built-in twisted belt external thread tubes, and it was found that Cu-water nanofluids show the best heat transfer performance. Yang et al. [15] experimentally investigated the flow and heat transfer characteristics of Cu-water and Cu-viscoelastic fluid nanofluids in a smooth tube, and the results showed that Cu-viscoelastic fluid nanofluids have a higher heat transfer performance than viscoelastic base fluid but a lower flow resistance than Cu-water nanofluids. Abdolbaqi et al. [16] experimentally studied the heat transfer enhancement of TiO_2-BioGlycol/water nanofluids in flat tubes and established a new correlation between the heat transfer enhancement and the friction factor, and the results showed that the heat transfer performance of nanofluids is approximately 28.2% greater than the base fluid. Naphon [17] experimentally studied the heat transfer characteristics of TiO_2-water nanofluids in horizontal spirally coiled tubes, and it was found that heat transfer performance of nanofluids increases with the decreasing curvature and the increasing nanoparticle fraction. Shahrul et al. [18] and Kumar and Sonawane [19] experimentally investigated the heat transfer characteristics of three kinds of nanofluids (Al_2O_3-water, SiO_2-water, and ZnO-water) and two kinds of nanofluids (Fe_2O_3-water and Fe_2O_3-EG) in a shell and tube heat exchanger, and it was found that ZnO-water and Fe_2O_3-water nanofluids show the best heat transfer performance in their respective research. El-Maghlany et al. [20] experimentally investigated the heat transfer characteristics and pressure drop of Cu-water nanofluids in a horizontal double-tube heat exchanger, and the results showed that heat transfer enhancement of nanofluids increases with the nanoparticle fraction. Sundar et al. [21] experimentally studied the flow and heat transfer characteristics of Fe_3O_4-water nanofluids in a horizontal plain tube with return bend and wire coil inserts, and the results showed that heat transfer performance increases with the increasing nanoparticle fraction and decreasing p/d ratio of wire coil inserts. Above studies mainly focused on the heat transfer performance of nanofluids in the smooth tube, flat tube, spirally coiled tube, or tube with wire coil inserts.

In addition to above experimental studies, the forced convection heat transfer characteristics of nanofluids in spirally corrugated tubes are also investigated. Darzi et al. [22, 23] experimentally and numerically studied the turbulent heat transfer of Al_2O_3-water nanofluids in a helically corrugated tube, and the results showed that a better heat transfer performance is obtained than that in a plain tube. Darzi et al. [24] experimentally investigated the turbulent heat transfer characteristics of SiO_2-water nanofluids in helically corrugated tubes and discussed the effects of five pitches of corrugation on the heat transfer of corrugated tubes, and the results showed that the small pitch of corrugations can augment the heat transfer performance significantly. Park et al. [25] studied the heat transfer of thermochromic liquid crystals in a spirally fluted tube, and the results showed that the heat transfer enhancement ratio between the spirally fluted tube and the smooth tube at the low Reynolds number (30,000) is higher than that at high Reynolds numbers (50,000 and 70,000). Above researches mainly investigated the heat transfer and flow characteristics of nanofluids in spirally corrugated tubes. However, the comprehensive analysis for the thermo-hydraulic performance of nanofluids in the smooth tube and spirally fluted tube needs to be discussed further.

Above studies made a great contribution to the flow and heat transfer characteristics in the smooth tube, smooth tube with wire coil inserts, heat exchanger, spirally corrugated tube, and so on. The main novelty of this manuscript mainly includes the following: (1) a new method of testing the stability of nanofluids (transmittance method) is established by an ultraviolet spectrophotometer, which is different from the precipitation method widely adopted by the published references. The results of transmittance method are quantifiable while the results of precipitation method are less quantifiable; and (2) the comprehensive evaluations for the thermo-hydraulic performance of TiO_2-water nanofluids in the smooth tube and spirally fluted tube are discussed, which are less investigated. On an interesting note, it is found that nanofluids at the highest Reynolds number may not have the best thermo-hydraulic performance in the spirally fluted tube and there is a critical Reynolds number for the best thermo-hydraulic performance.

Methods

Nanofluid Preparation and Stability Study

TiO_2 is chosen as the nanoparticle, and water is selected as the base fluid. Figure 1 shows the TiO_2 nanoparticles. TiO_2-water nanofluids in the experiment are prepared by a two-step method, and Fig. 2 presents the details of the preparation process. For each of the sub-steps, mechanical stirring time is half an hour and the sonication time is 40 min. The mass fraction of the dispersant agent in the water is 6 wt%, and the pH value of nanofluid is 8. Table 1 presents the information of some materials in the preparation process of nanofluids. From Fig. 1, it is found that the nanoparticles easily aggregate

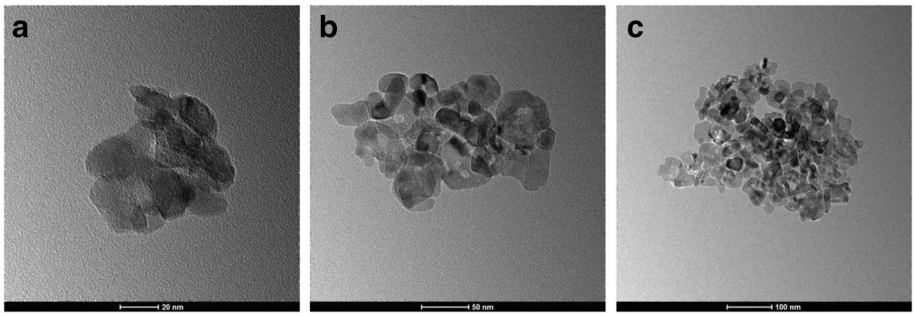

Fig. 1 Morphology of TiO_2 nanoparticles. TEM images of TiO_2 nanoparticles: **a** ⟷ 20 nm, **b** ⟷ 50 nm, and **c** ⟷ 100 nm

together. Hence, the stability of nanofluids is investigated using the precipitation method widely adopted by the published references. The stability of TiO_2-water nanofluids with various mass fractions (0.1, 0.3, and 0.5 wt%) at different quiescent times is studied in Fig. 3, which shows that the stability of nanofluids 72 h later is still good.

In order to further check the stability of nanofluids, a new method of testing the stability of nanofluids (transmittance method) is established by an ultraviolet spectrophotometer in this paper. Figure 4 shows the transmittance (τ) changes of TiO_2-water nanofluids (ω = 0.3%) with the quiescent time. The effects of different doses (M) of dispersant agent and different pH values on the stability of nanofluids are investigated. As we know, if nanoparticles uniformly distribute in the water, nanofluids will reflect the most light, resulting in nanofluids having a high reflectance and a low transmittance. It can be found from Fig. 4 that nanofluids (ω = 0.3%) with M = 6 wt% and pH = 8 have the lowest transmittance. Nanofluids with other mass fractions (ω = 0.1% and ω = 0.5%) are all prepared at M = 6 wt% and pH = 8 in this paper, and the transmittance change trends of nanofluids with ω = 0.1% and ω = 0.5% are the same with the nanofluids with ω = 0.3%. Hence, the good stability of nanofluids prepared in this paper can be guaranteed. In addition, following the investigation of the effects of dispersant agent and pH on the thermal conductivity and viscosity of water, a small influence on them due to the little dispersant agent and NaOH is found.

Figure 5 shows the thermal conductivities and dynamic viscosities of TiO_2-water nanofluids at different temperatures and shear rates. It is found that the thermal conductivity of water in this paper has a good agreement with Maxwell [26]. It can be found that the thermal conductivity increases with the nanoparticle mass fraction and the thermal conductivity of nanofluids increases by 0.17–1.6% compared with water due to the high thermal conductivity of nanoparticles. Also, it is found that the thermal conductivity increases with the temperature, because high temperature enhances the Brownian motion of nanoparticles and improves the thermal conductivity of nanofluids. In addition to the conclusions of thermal conductivity, it can be found that the dynamic viscosity increases with the shear rate at the initial stage and keeps constant with the increasing shear rate and the viscosity of nanofluids increases by 2.5–13.6% compared with water. It is because that a small shear force added in the nanofluids at the initial stage breaks the equilibrium of the flow field and causes an increase in dynamic viscosity (shear-thickening behavior). The dynamic viscosity is constant when the flow field reaches a steady state again, which has a good agreement with the characteristics of Newtonian fluid.

Experimental System

An experimental system for the flow and heat transfer characteristics of TiO_2-water nanofluids in a spirally fluted tube is established. Figure 6 represents the schematic diagram of the experimental system. The experimental system mainly includes the heat transfer test section, flow resistance test section, temperature control sink, and pump. The spirally fluted tube is heated by a resistance wire connected to a DC power. Outer wall temperature of the spirally fluted tube is obtained by ten

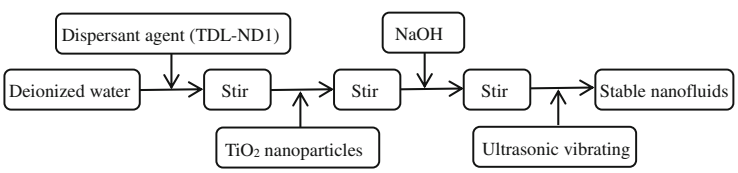

Fig. 2 Preparation of nanofluids. Preparation process of TiO_2-water nanofluids by a two-step method

Table 1 Information of materials. Information of some materials in the preparation of nanofluids

Materials	Manufacturer	Properties
TiO_2 nanoparticles	Nanjing Tansail Advanced Materials Co., Ltd.	Type: TTP-A10; Crystal form: anatase; Particle diameter: 10 nm
Base fluid (deionized water)	Prepared by ultrapure water device	Resistivity: 16–18.2 MΩ cm@25 °C
Dispersant agent	Nanjing Tansail Advanced Materials Co., Ltd.	Type: TDL-ND1; Element: macromolecule polymers; Scope of application: water or solvent (base fluid)

T-type thermocouples which are uniformly distributed in the surface of the spirally fluted tube. Outlet temperature and inlet temperature of nanofluids of the spirally fluted tube are measured by two K-type thermocouples. All thermocouples are connected to a data acquisition instrument (Agilent 34972A). The flow resistance is measured by a differential pressure instrument.

The detailed diagram of the spirally fluted tube is shown in Fig. 7. For the smooth tube and spirally fluted tube, the materials are all stainless steel, the equivalent diameters are the same, the lengths are all 1200 mm, the test sections are all the middle section 1000 mm of the tube, and 100 mm section is left at each end of the tube in order to avoid the entrance effect.

Calculation Equations

The heating power is supplied by a DC power:

$$Q_0 = UI \tag{1}$$

where Q_0 is the heating power, U is the voltage, and I is the electric current.

The heat absorbed by fluid is calculated as follows:

$$Q_f = c_p q_m (T_{out} - T_{in}) \tag{2}$$

where Q_f is the heat absorbed by fluid, c_p is the specific heat of fluid, q_m is the mass flow rate, and T_{out} and T_{in} are the outlet temperature and inlet temperature of fluid.

Heat capacity is given as follows:

$$c_p = \frac{(1-\phi)(\rho c_p)_{bf} + \phi(\rho c_p)_p}{(1-\phi)\rho_{bf} + \phi\rho_p} \tag{3}$$

where c_p is the heat capacity of nanofluids, ϕ is the nanoparticle volume fraction, the subscript "bf" represents the base fluid, and the subscript "p" represents the nanoparticles.

The average temperature of fluid is calculated as follows:

$$T_f = (T\text{out} + T\text{in})/2 \tag{4}$$

where T_f is the average temperature of fluid in the tube.

The outer wall average temperature of the tube is shown as follows:

$$T_{ow} = \left[\sum_{i=1}^{10} T\text{w}(i)\right]/10 \tag{5}$$

where T_{ow} is the outer wall average temperature of the tube, $T\text{w}(i)$ is the temperature of thermocouples attached to the outer wall of tube, and there are ten thermocouples attached uniformly to the outer wall of tube.

The internal wall average temperature of the tube can be calculated as follows:

$$T_{iw} = T_{ow} - \frac{Q_f \ln(ro/ri)}{2\pi\lambda l}, (i = 1, 2, 3...10) \tag{6}$$

where T_{iw} is the internal wall average temperature of the tube, ro and ri are the external radius and internal radius of tube, λ is the thermal conductivity of tube, and l is the length of tube.

The convective heat transfer coefficient is calculated as follows:

$$h_f = \frac{Q_f}{\pi d_e l (T_{iw} - T_f)} \tag{7}$$

where h_f is the convective heat transfer coefficient and d_e is the equivalent diameter of the tube.

The Nusselt number is calculated as follows:

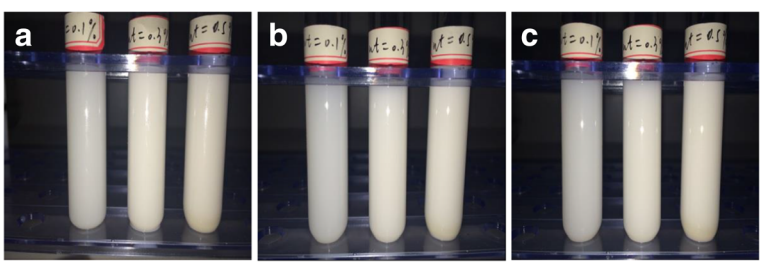

Fig. 3 Stability observation of nanofluids. TiO_2-water nanofluids at different quiescent times: **a** t = 0 h, **b** t = 48 h, and **c** t = 72 h

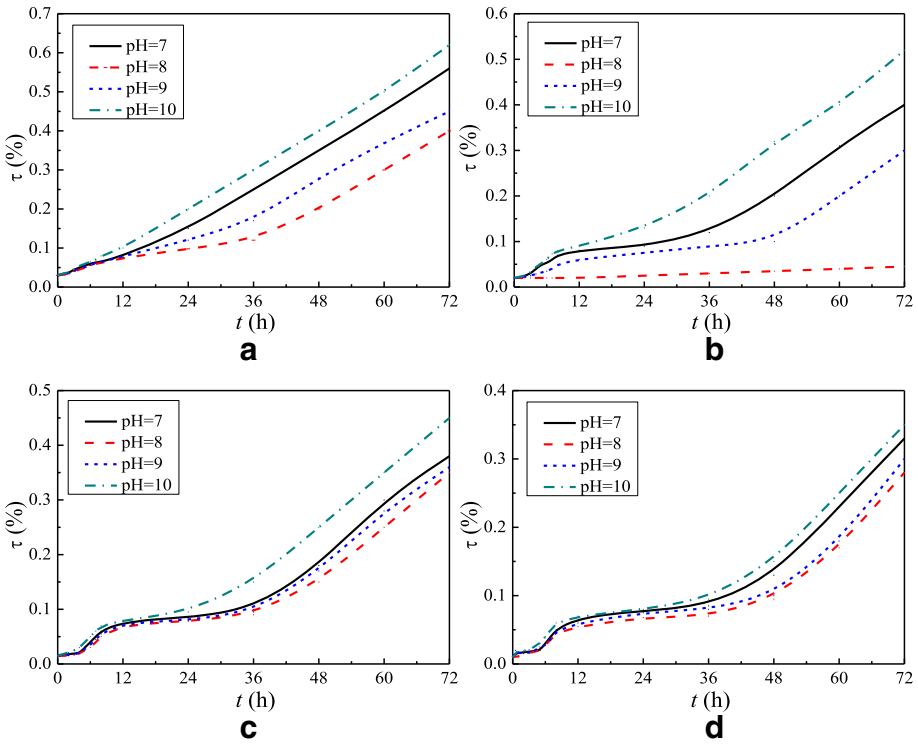

Fig. 4 Transmittance (τ) of nanofluid (ω = 0.3%). Transmittance changes with quiescent time of TiO_2-water nanofluid (ω = 0.3%) with different doses (M) of dispersant agent: **a** M = 5 wt%, **b** M = 6 wt%, **c** M = 7 wt%, and **d** M = 8 wt%

$$Nu = \frac{h_f d_e}{\lambda_f} \tag{8}$$

where Nu is the Nusselt number and λ_f is the thermal conductivity of fluid in the tube measured by a thermal conductivity measuring instrument.

The Reynolds number is shown as follows:

$$\mathrm{Re} = \rho u d_e / \mu_f \tag{9}$$

where Re is the Reynolds number, ρ is the density of fluid, u is the velocity of fluid, and μ_f is the dynamic viscosity of fluid measured by a super rotational rheometer.

Density of nanofluids is shown as follows:

$$\rho = (1-\phi)\rho_{bf} + \phi\rho_p \tag{10}$$

where ρ is the density of the nanofluids, ϕ is the volume fraction of the nanoparticles, ρ_{bf} is the density of water, and ρ_p is the density of the nanoparticles.

Frictional resistance coefficient of fluid is presented as follows:

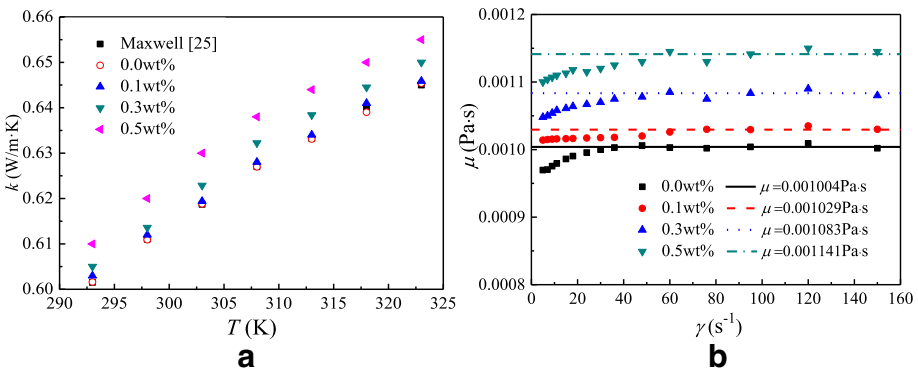

Fig. 5 Thermal conductivities and dynamic viscosities. Thermal conductivities and dynamic viscosities of TiO_2-water nanofluids at different temperatures and shear rates. **a** Thermal conductivities **b** Dynamic viscosity

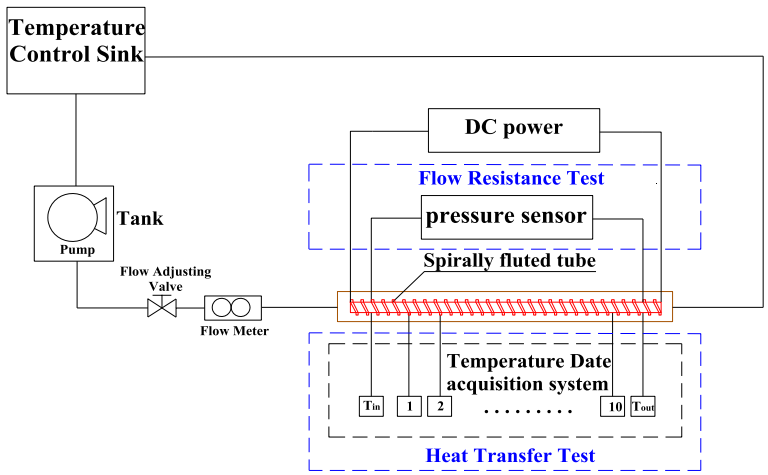

Fig. 6 Experimental system. Schematic diagram of experimental system

$$f = \frac{2de}{\rho u^2} \cdot \frac{\Delta p}{\Delta l} \tag{11}$$

where f is the frictional resistance coefficient and $\frac{\Delta p}{\Delta l}$ is the pressure drop per unit length.

The equation of the comprehensive evaluation between heat transfer and flow resistance is shown as follows [27]:

$$\varsigma = \left(\frac{Nu}{Nu_{(\text{bf+smooth tube})}}\right) / \left(\frac{f}{f_{(\text{bf+smooth tube})}}\right)^{\frac{1}{3}} \tag{12}$$

where ς is the comprehensive evaluation index.

Uncertainty Analysis

Experimental errors are caused by the accuracies of the equipment in the experimental system. The corresponding error equations are shown as follows:

$$\frac{\delta Nu}{Nu} = \sqrt{\left(\frac{\delta Q_f}{Q_f}\right)^2 + \left(\frac{\delta T}{T}\right)^2} \tag{13}$$

$$\frac{\delta f}{f} = \sqrt{\left(\frac{\delta p}{p}\right)^2 + \left(\frac{\delta l}{l}\right)^2 + \left(\frac{\delta q\text{m}}{q\text{m}}\right)^2} \tag{14}$$

where the accuracy of DC power is ± 5.0%, the accuracy of thermocouple is ± 0.1%, and the error of the Nusselt number can be obtained from Eq. (13) and is approximately ± 5.0%. The accuracy of pressure transducer is ± 0.5%, the accuracy of length is ± 0.1%, the accuracy of mass flow rate is ± 1.06%, and the error of frictional resistance coefficient can be obtained from Eq. (14) and is approximately ± 1.29%.

Results and Discussions

Experimental System Validation

Before the experimental study on nanofluids, the experimental system validation is necessary. Water is chosen as the heat transfer medium. Nusselt numbers and frictional resistance coefficients between the experimental results of this paper and the results of published literatures are shown in Figs. 8 and 9. It can be found from Figs. 8 and 9 that Nusselt numbers and frictional resistance coefficients at different Reynolds numbers have a good agreement with the results of the published literatures [28, 29] and [30, 31] respectively. The max errors for Nusselt numbers and frictional resistance coefficients at laminar flow and turbulent flow are approximately 3.5, 2.8, 2.1, and 2.1%, respectively, which verify the accuracy and reliability of the experimental system. Also, it is found that the results of Dittus-Boelter in Fig. 8b are higher than the real results under the transitional flow

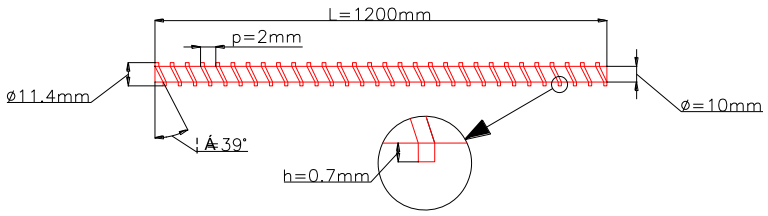

Fig. 7 Spirally fluted tube. Detailed diagram of the spirally fluted tube

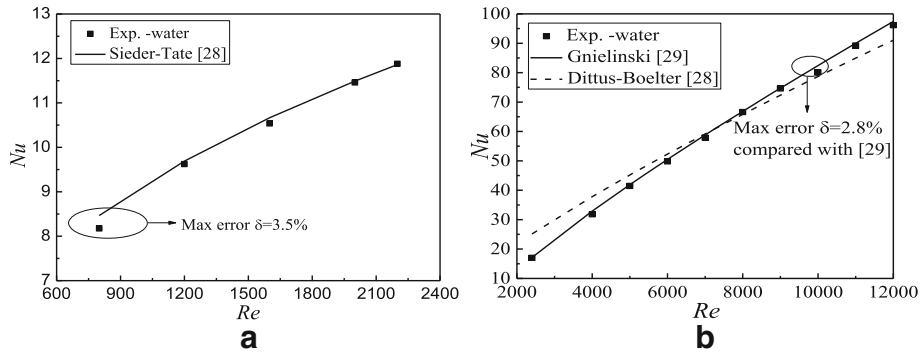

Fig. 8 Heat transfer characteristics validation. Comparison of Nusselt numbers between the experimental results and the results of literatures. **a** Laminar flow **b** Turbulent flow

because the empirical formula only can be applied to the strong turbulence zone, which agrees with the results of literature [28]. It proves the validity of the results in this paper further.

Experimental Results and Discussions

The flow and heat transfer characteristics of TiO_2-water nanofluids in the smooth tube are investigated. Figure 10 presents the Nusselt numbers of the smooth tube filled with nanofluids at different Reynolds numbers. For laminar flow and turbulent flow, the Nusselt number increases with the Reynolds number and nanoparticle mass fraction. The turbulivity of fluid increases with the Reynolds number, which reduces the laminar boundary layer and improves the heat transfer. Adding more nanoparticles into the base fluid causes the increase of whole thermal conductivity, which also improves the heat transfer. In addition, it is suggested [32, 33] that other factors including the increase of Brownian motion of nanoparticles, reduction of the contact angles, non-uniform shear rate, particle shape, and aggregation also have great influence in the heat transfer enhancement. In the previous published paper [11], the effects of Brownian force and particle size on heat transfer enhancement were discussed. It was found that Brownian force is the biggest force of the interaction forces between nanoparticles, which is advantageous to the heat transfer enhancement, and the small particle size is also advantageous to the heat transfer enhancement. It is found from Fig. 10a that the heat transfer enhancement ratio from water to $\omega = 0.1$ wt% nanofluids shows the largest one, but the heat transfer enhancement ratio of nanofluids from $\omega = 0.1$ wt% to $\omega = 0.3$ wt% begins to decline, and the heat transfer enhancement ratio of nanofluids from $\omega = 0.3$ wt% to $\omega = 0.5$ wt% witnesses the smallest one. As Fig. 5 shows, the thermal conductivity and viscosity of nanofluids increase by 0.17–1.6% and 2.5–13.6% compared with water, respectively. For the laminar flow, the effects of viscosity on heat transfer are small due to the low velocity and few nanoparticles, and then the thermal conductivity plays a major role from water to $\omega = 0.1$ wt% nanofluids. However, with an increase in nanoparticle fraction, it shows a more dramatic increase in viscosity compared with the increase in the thermal conductivity, which causes the heat transfer enhancement

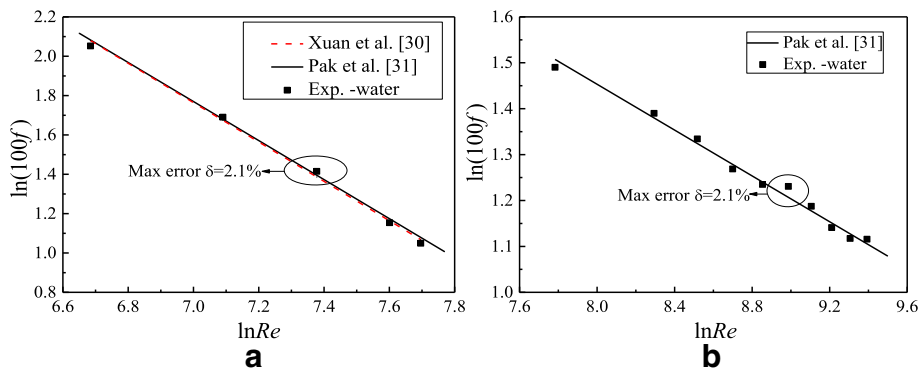

Fig. 9 Flow characteristics validation. Comparison of frictional resistance coefficients between the experimental results and the results of literatures. **a** Laminar flow **b** Turbulent flow

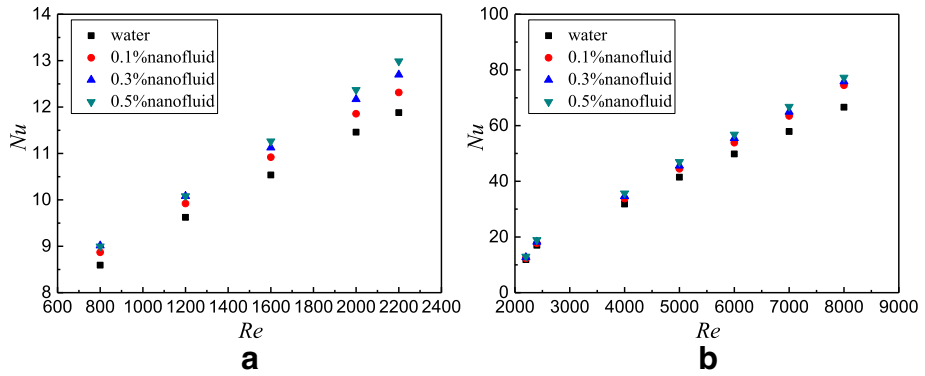

Fig. 10 Nusselt numbers in the smooth tube. Nusselt numbers of the smooth tube filled with nanofluids at different Reynolds numbers. **a** Laminar flow **b** Turbulent flow

ratio to decrease. For the turbulent flow, it is found that the heat transfer enhancements of nanofluids with different nanoparticle mass fractions are close. This is because the turbulence plays a major role in the heat transfer enhancement, and the effect of nanoparticle mass fraction becomes small. Also, it can be found that nanofluids show a larger heat transfer enhancement ratio in laminar flow compared with that in turbulent flow. Nanoparticle mass fraction plays a major role in the heat transfer enhancement in laminar flow, and it shows a large heat transfer enhancement with the increasing nanoparticle mass fraction. However, the effect of nanoparticle mass fraction on heat transfer enhancement becomes small in turbulent flow, and the turbulence intensity plays a major role; hence, it shows a smaller heat transfer enhancement ratio with the increasing nanoparticle mass fraction in turbulent flow compared with that in laminar flow.

Based on the data of Fig. 10, Fig. 11 shows the Nusselt number ratios of nanofluids to the water in the smooth tube. It can be found that TiO_2-water nanofluids with $\omega = 0.5$ wt%, $\omega = 0.3$ wt%, and $\omega = 0.1$ wt% enhance the heat transfer by 11.2, 7.4, and 4.5% for laminar flow and 16.1, 13.9, and 11.9% for turbulent flow at best compared with water in the smooth tube, respectively.

In addition to the study on the heat transfer characteristics of TiO_2-water nanofluids in the smooth tube, the flow characteristics are also investigated. Figure 12 presents the frictional resistance coefficients and pressure drop of the smooth tube filled with nanofluids. From Fig. 12, it is found that the frictional resistance coefficient decreases with the Reynolds number because the increasing Reynolds number causes the increase of velocity, which is inversely proportional to the frictional resistance coefficient according to the Eqs. (9) and (11). It is found that the pressure drop decreases with the frictional resistance coefficient because the pressure drop is proportional to the Reynolds number but the frictional resistance coefficient is inversely proportional to the Reynolds number. Hence, the pressure drop is inversely proportional to the frictional resistance coefficient. Also, it can be found from Fig. 12 that the frictional resistance coefficient increases with nanoparticle mass fraction but the increase is small between different nanoparticle mass fractions. For TiO_2-water nanofluids with $\omega = 0.5$ wt%, $\omega = 0.3$ wt%, and $\omega = 0.1$ wt% in the smooth tube, a maximum enhancement of 7.9, 5.2, and 3.0% at laminar flow and 2.5, 1.5, and 0.6% at turbulent flow occurs in the frictional resistance coefficients compared with water in the smooth tube, respectively. Adding nanoparticles into water causes the increase of viscosity which is proportional to the frictional resistance coefficient. However, the frictional resistance is mainly caused by the screw structure of the spirally fluted tube, and the effect of nanoparticles on the frictional resistance is much smaller than that of the screw structure, which causes a small difference between different nanoparticle mass fractions.

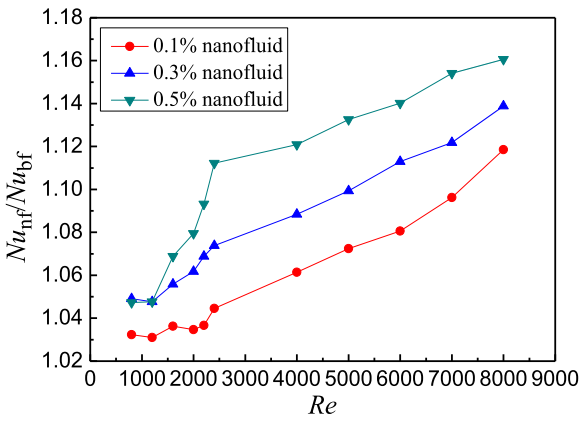

Fig. 11 Nusselt number ratios in the smooth tube. Nusselt number ratios between nanofluids and base fluid in the smooth tube

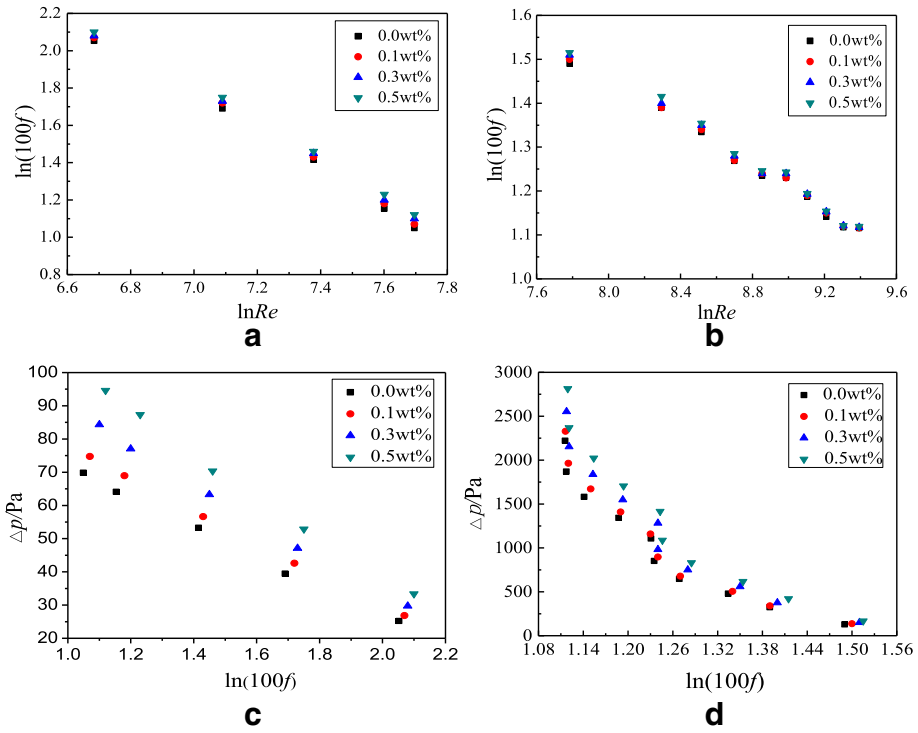

Fig. 12 Frictional resistance coefficients and pressure drop in the smooth tube. Frictional resistance coefficients and pressure drop of the smooth tube filled with nanofluids. Frictional resistance coefficients: **a** laminar flow and **b** turbulent flow; pressure drop: **c** laminar flow and **d** turbulent flow

Above studies are on smooth tube, and the flow and heat transfer characteristics of water and TiO_2-water nanofluids in the spirally fluted tube will be investigated in the following text. Figure 13 presents the Nusselt numbers of the spirally fluted tube filled with TiO_2-water nanofluids at different Reynolds numbers. It obtains a similar conclusion in the spirally fluted tube (Fig. 13) similar to that in the smooth tube (Fig. 10). It is found that the Nusselt number increases with the Reynolds number and nanoparticle mass fraction. The differences between the spirally fluted tube and smooth tube are that there is a larger heat transfer enhancement in the spirally fluted tube than that in the smooth tube, which is due to the screw structure of the spirally fluted tube.

Based on the data of Fig. 13, Fig. 14 shows the Nusselt number ratios of nanofluids to the water in the spirally fluted tube. Figure 14 shows that TiO_2-water nanofluids with $\omega = 0.5$ wt%, $\omega = 0.3$ wt%, and $\omega = 0.1$ wt% can enhance the heat transfer by 14.7, 12.6, and 11.3% for laminar flow and 42.8, 35.4, and 24.6% for turbulent flow at best compared with water in the spirally fluted tube, respectively. There is a larger increase in heat transfer for turbulent flow than that for laminar flow.

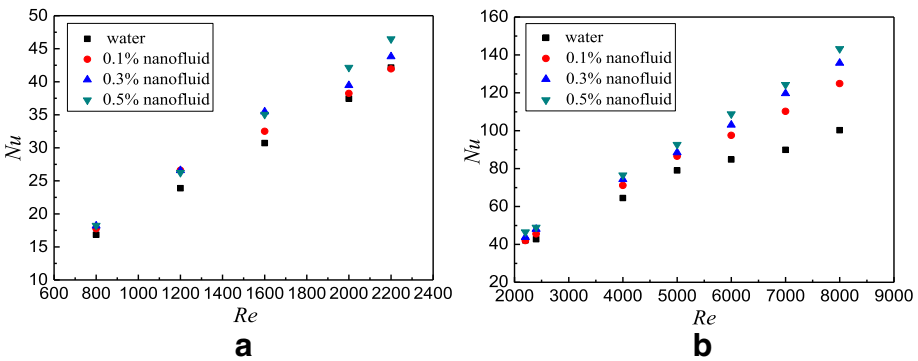

Fig. 13 Nusselt numbers in the spirally fluted tube. Nusselt numbers of the spirally fluted tube filled with nanofluids at different Reynolds numbers. **a** Laminar flow **b** Turbulent flow

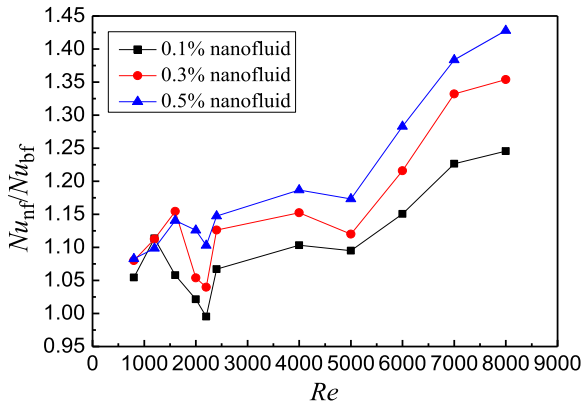

Fig. 14 Nusselt number ratios in the spirally fluted tube. Nusselt number ratios between nanofluids and base fluid in the spirally fluted tube

The flow characteristics of TiO_2-water nanofluids in the spirally fluted tube are also studied. Figure 15 presents the frictional resistance coefficients and pressure drop of the spirally fluted tube filled with nanofluids, which shows that the frictional resistance coefficient decreases with the Reynolds number and increases with the nanoparticle mass fraction, and the pressure drop decreases with the frictional resistance coefficient. The reasons are similar to that in the smooth tube (Fig. 12c, d). TiO_2-water nanofluids with $\omega = 0.5$ wt%, $\omega = 0.3$ wt%, and $\omega = 0.1$ wt% can enhance the frictional resistance coefficients by 20.2, 16.5, and 12.5% for laminar flow and 10.5, 7.7, and 2.0% for turbulent flow at best compared with water in the spirally fluted tube, respectively. There is a smaller increase in frictional resistance coefficients for turbulent flow than that for laminar flow.

The heat transfer characteristics of TiO_2-water nanofluids in the smooth tube and spirally fluted tube are investigated in this paper separately. Figure 16 shows the comparison of Nusselt numbers between the smooth tube and the spirally fluted tube filled with nanofluids at different Reynolds numbers. It can be found that TiO_2-water nanofluids with $\omega = 0.5$ wt%, $\omega = 0.3$ wt%, and $\omega = 0.1$ wt% in the spirally fluted tube can enhance the heat transfer by 257.9, 245.1, and 240.7% at best compared with TiO_2-water nanofluids in the smooth tube, respectively. Also, TiO_2-water nanofluids with $\omega = 0.5$ wt%, $\omega = 0.3$ wt%, and $\omega = 0.1$ wt% in the spirally fluted tube can enhance the heat transfer by 291.3, 268.8, and 253.1% at best compared with water in the smooth tube, respectively. TiO_2-water nanofluids in the spirally fluted tube have a larger enhancement than that in the smooth tube.

In order to synthetically analyze the thermo-hydraulic performance of TiO_2-water nanofluids in the smooth

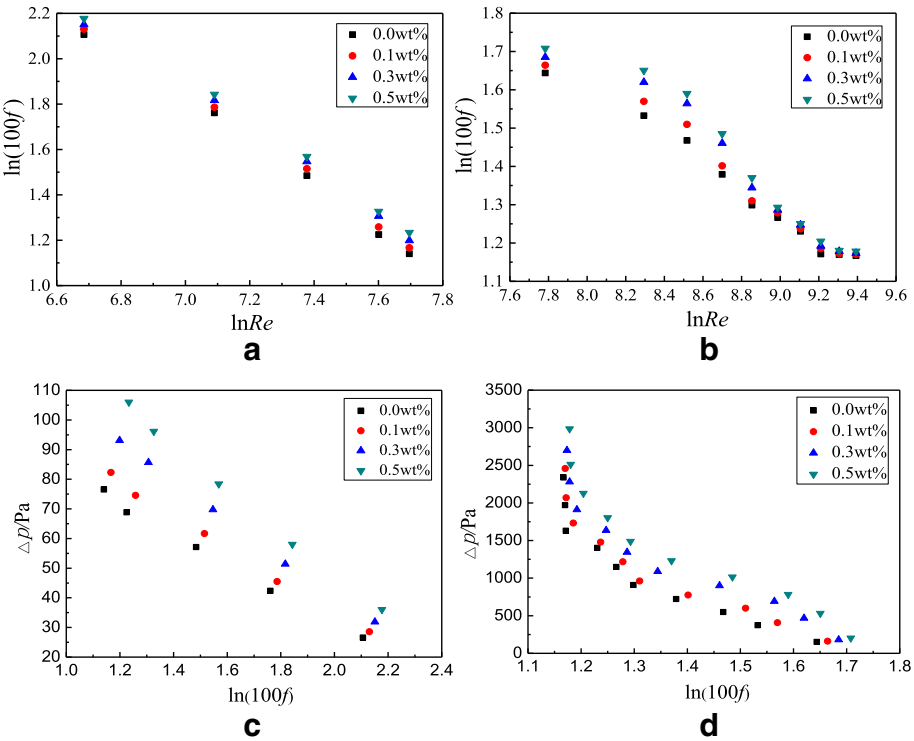

Fig. 15 Frictional resistance coefficients and pressure drop in the spirally fluted tube. Frictional resistance coefficients of the spirally fluted tube filled with nanofluids. Frictional resistance coefficients: **a** laminar flow and **b** turbulent flow; pressure drop: **c** laminar flow and **d** turbulent flow

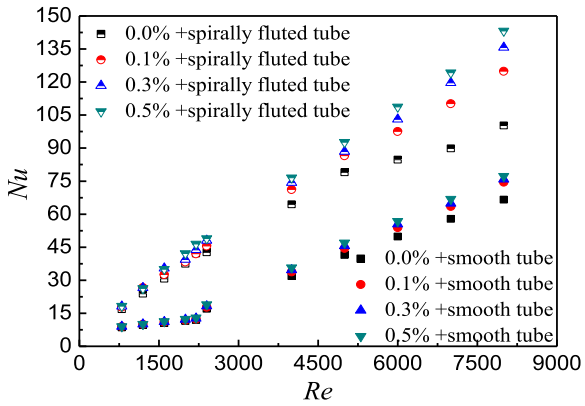

Fig. 16 Comparison of Nusselt numbers in two tubes. Comparison of Nusselt numbers between the smooth tube and spirally fluted tube filled with nanofluids at different Reynolds numbers

tube and spirally fluted tube, Fig. 17 presents the comprehensive analysis of nanofluids in the smooth tube and the spirally fluted tube based on the Eq. (12). It can be found that the highest comprehensive evaluation index ξ for spirally fluted tube is about at Re = 2300 which is the critical Reynolds number between laminar flow and turbulent flow. The increases of the Nusselt number and frictional resistance coefficients are mainly due to the nanoparticles, the Reynolds number, and the screw structure of spirally fluted tube. For spirally fluted tube, due to the screw structure, the increase of the Nusselt number is larger than the increase of frictional resistance coefficients at small Reynolds number ($Re \leq 2300$); conversely, the increase of the Nusselt number is smaller than the increase of frictional resistance coefficients at big Reynolds number ($Re > 2300$). Also, the comprehensive evaluation index ξ for the smooth tube increases with the Reynolds number. The increase of the Nusselt number is always larger than the increase of frictional resistance coefficients because the smooth tube has no

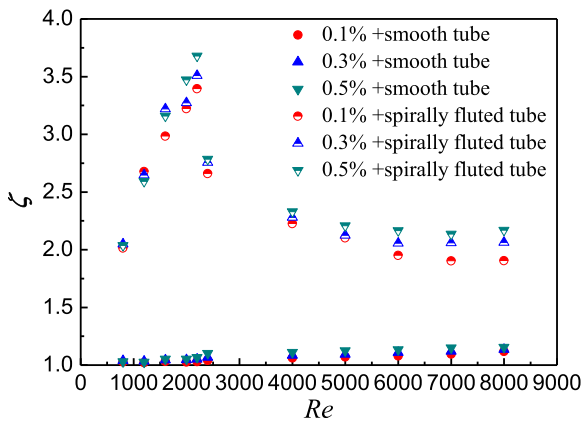

Fig. 17 Comprehensive analysis of the two tubes. Comprehensive analysis of nanofluids in the smooth tube and the spirally fluted tube

screw structure. The conclusions of Fig. 17 are very important for the choices of tubes and Reynolds numbers in the heat-exchange equipment considering the comprehensive evaluation of the thermo-hydraulic performance. For the smooth tube, the higher Reynolds number can be chosen due to the factor that the thermo-hydraulic index always increases with the Reynolds number. While for the spirally fluted tube, the appropriate Reynolds number for the highest thermo-hydraulic index is about 2300.

Conclusions

The flow and heat transfer characteristics of TiO_2-water nanofluids in a spirally fluted tube are experimentally studied. Some conclusions are obtained as follows:

(1) TiO_2-water nanofluids with different nanoparticle mass fractions are prepared, and TiO_2-water nanofluids with M = 6 wt% and pH = 8 have the lowest transmittance and show the best stability.
(2) For TiO_2-water nanofluids in the spirally fluted tube, there is a larger increase in heat transfer and a smaller increase in frictional resistance coefficients for turbulent flow than that for laminar flow.
(3) TiO_2-water nanofluids in the spirally fluted tube have a larger enhancement than that in the smooth tube. TiO_2-water nanofluids in the spirally fluted tube can enhance the heat transfer by 257.9% at best compared with that in the smooth tube.
(4) The highest comprehensive evaluation indexes of TiO_2-water nanofluids in the spirally fluted tube and smooth tube are different. For the spirally fluted tube, the highest comprehensive evaluation index ξ is at Re = 2300 which is the critical Reynolds number between the laminar flow and the turbulent flow. For the smooth tube, the comprehensive evaluation index ξ increases with the Reynolds number.

Acknowledgements

This work is financially supported by the "National Natural Science Foundation of China" (Grant No. 51606214) and "the Fundamental Research Funds for the Central Universities" (Grant No. 2015XKMS063).

Authors' Contributions

CQ participated in the design of the experiment set, carried out the experiment of nanofluid, and drafted the manuscript. CYL carried out the experiment of nanofluid and processed the data. GQW carried out the experiment of nanofluid. All authors read and approved the final manuscript.

Competing Interests

The authors declare that they have no competing interests.

Publisher's Note

Received: 13 April 2017 Accepted: 19 August 2017
Published online: 02 September 2017

References

1. Li H, Wang L, He Y, Hu Y, Zhu J, Jiang B (2015) Experimental investigation of thermal conductivity and viscosity of ethylene glycol based ZnO nanofluids. Appl Therm Eng 88:363–368
2. Yang JC, Li FC, Zhou WW, He YR, Jiang BC (2012) Experimental investigation on the thermal conductivity and shear viscosity of viscoelastic-fluid-based nanofluids. Int J Heat Mass Transf 55(11):3160–3166
3. Li FC, Yang JC, Zhou WW, He YR, Huang YM, Jiang BC (2013) Experimental study on the characteristics of thermal conductivity and shear viscosity of viscoelastic-fluid-based nanofluids containing multiwalled carbon nanotubes. Thermochim Acta 556:47–53
4. Huang J, He Y, Wang L, Huang Y, Jiang B (2017) Bifunctional au@TiO_2 core–shell nanoparticle films for clean water generation by photocatalysis and solar evaporation. Energy Convers Manag 132:452–459
5. Chen M, He Y, Huang J, Zhu J (2017) Investigation into au nanofluids for solar photothermal conversion. Int J Heat Mass Transf 108:1894–1900
6. Hu Y, Li H, He Y, Liu Z, Zhao Y (2017) Effect of nanoparticle size and concentration on boiling performance of SiO_2 nanofluid. Int J Heat Mass Transf 2017(107):820–828
7. Li H, He Y, Hu Y, Jiang B, Huang Y (2015) Thermophysical and natural convection characteristics of ethylene glycol and water mixture based ZnO nanofluids. Int J Heat Mass Transf 91:385–389
8. Hu Y, He Y, Qi C, Jiang BC, Schlaberg HI (2014) Experimental and numerical study of natural convection in a square enclosure filled with nanofluid. Int J Heat Mass Transf 78:380–392
9. He Y, Qi C, Hu Y, Qin B, Li F, Ding Y (2011) Lattice Boltzmann simulation of alumina-water nanofluid in a square cavity. Nanoscale Res Lett 6(1):184
10. Qi C, He Y, Hu Y, Yang J, Li F, Ding Y (2011) Natural convection of Cu-gallium nanofluid in enclosures. J Heat Transf 133(12):122504
11. Qi C, Liang L, Rao Z (2016) Study on the flow and heat transfer of liquid metal based nanofluid with different nanoparticle radiuses using two-phase lattice Boltzmann method. Int J Heat Mass Transf 94:316–326
12. Qi C, He Y, Yan S, Tian F, Hu Y (2013) Numerical simulation of natural convection in a square enclosure filled with nanofluid using the two-phase lattice Boltzmann method. Nanoscale Res Lett 8(1):56–71
13. Sun B, Yang A, Yang D (2017) Experimental study on the heat transfer and flow characteristics of nanofluids in the built-in twisted belt external thread tubes. Int J Heat Mass Transf 107:712–722
14. Sun B, Zhang Z, Yang D (2016) Improved heat transfer and flow resistance achieved with drag reducing Cu nanofluids in the horizontal tube and built-in twisted belt tubes. Int J Heat Mass Transf 95:69–82
15. Yang JC, Li FC, He YR, Huang YM, Jiang BC (2013) Experimental study on the characteristics of heat transfer and flow resistance in turbulent pipe flows of viscoelastic-fluid-based Cu nanofluid. Int J Heat Mass Transf 62:303–313
16. Abdolbaqi MK, Mamat R, NAC S, Azmi WH, Selvakumar P (2017) Experimental investigation and development of new correlations for heat transfer enhancement and friction factor of BioGlycol/water based TiO_2 nanofluids in flat tubes. Int J Heat Mass Transf 108:1026–1035
17. Naphon P (2016) Experimental investigation the nanofluids heat transfer characteristics in horizontal spirally coiled tubes. Int J Heat Mass Transf 93: 293–300
18. Shahrul IM, Mahbubul IM, Saidur R, Sabri MFM (2016) Experimental investigation on Al_2O_3–W, SiO_2–W and ZnO–W nanofluids and their application in a shell and tube heat exchanger. Int J Heat Mass Transf 97:547–558
19. Kumar N, Sonawane SS (2016) Experimental study of Fe_2O_3/water and Fe_2O_3/ethylene glycol nanofluid heat transfer enhancement in a shell and tube heat exchanger. Int Commun Heat Mass Transfer 78:277–284
20. El-Maghlany WM, Hanafy AA, Hassan AA, El-Magid M.A. (2016) Experimental study of Cu–water nanofluid heat transfer and pressure drop in a horizontal double-tube heat exchanger. Exp Thermal Fluid Sci 78:100–111
21. Sundar LS, Bhramara P, NTR K, Singh MK, Sousa ACM (2017) Experimental heat transfer, friction factor and effectiveness analysis of Fe_3O_4 nanofluid flow in a horizontal plain tube with return bend and wire coil inserts. Int J Heat Mass Transf 109:440–453
22. Darzi AAR, Farhadi M, Sedighi K (2014) Experimental investigation of convective heat transfer and friction factor of Al_2O_3/water nanofluid in helically corrugated tube. Exp Thermal Fluid Sci 57:188–199
23. Darzi AAR, Farhadi M, Sedighi K, Aallahyari S, Delavar MA (2013) Turbulent heat transfer of Al_2O_3–water nanofluid inside helically corrugated tubes: numerical study. Int Commun Heat Mass Transfer 41:68–75
24. Darzi AAR, Farhadi M, Sedighi K, Shafaghat R, Zabihi K (2012) Experimental investigation of turbulent heat transfer and flow characteristics of SiO_2/water nanofluid within helically corrugated tubes. Int Commun Heat Mass Transfer 39(9):1425–1434
25. Park HJ, Lee DH, Ahn SW (2013) Study of local heat transfer in a spirally fluted tube. Int J Therm Sci 64:257–263
26. Maxwell JC (1873) A treatise on electricity and magnetism. Clarendon Press, London, pp 10–15
27. Qiu L, Deng H, Sun J, Tao Z, Tian S (2013) Pressure drop and heat transfer in rotating smooth square U-duct under high rotation numbers. Int J Heat Mass Transf 66:543–552
28. Yang SM, Tao WQ (2012) Heat transfer, 4th edn. Higher Education Press, Beijing (in Chinese)
29. Gnielinski V (1976) New equations for heat and mass-transfer in turbulent pipe and channel flow. Int Chem Eng 16(2):359–368
30. Xuan Y, Roetzel W (2000) Conceptions for heat transfer correlation of nanofluids. Int J Heat Mass Transf 43(19):3701–3707
31. Pak BC, Cho YI (1998) Hydrodynamic and heat transfer study of dispersed fluids with submicron metallic oxide particles. Exp Heat Transfer 11(2):151–170
32. Ebrahimnia-Bajestan E, Moghadam MC, Niazmand H, Daungthongsuk W, Wongwises S (2016) Experimental and numerical investigation of nanofluids heat transfer characteristics for application in solar heat exchangers. Int J Heat Mass Transf 92:1041–1052
33. Chen H, Yang W, He Y, Ding Y, Zhang L, Tan C, Lapkin AA, Bavykin DV (2008) Heat transfer and flow behaviour of aqueous suspensions of titanate nanotubes (nanofluids). Powder Technol 183(1):63–72